Electronic Journal «Technical Acoustics»
http://www.ejta.org

2013, 5

Thanh C Nguyen[1], Loan T Bui[2], Nghia H Tran[1], Victor Frenkel[2]

[1]*Department of Electrical Engineering, Catholic University of America, Washington, DC*
[2]*Department of Biomedical Engineering, Catholic University of America, Washington, DC*
E-mail: frenkel@cua.edu

Calibrating therapeutic ultrasound transducers: corrections for the effects of acoustic cavitation and acoustic streaming

Received 01.01.2013, published 19.06.2013

Commercial ultrasound power meters based on the radiation force technique are ubiquitously used in both the clinic and in laboratory settings for calibrating therapeutic ultrasound transducers. Despite their popularity, these devices are inherently inaccurate in that they do not compensate for the effects of acoustic cavitation and acoustic streaming. These factors can alter the displacement generated on the meter's target, and hence the power being sensed. In the present study we built a low cost power meter comprised of a non-reflecting target suspended from an analytical balance in a water tank. Investigations in to the effects of cavitation and streaming were performed, where the former was shown to significantly lower the measured power and the latter was shown to increase it. Both effects were found to be proportional to the applied power as predicted by theory. A modified device was then constructed, where an acoustic permeable membrane was positioned directly over the target and shown to effectively eliminate the streaming effect. For the effects of cavitation, a pair of ultrasound transmitting and receiving transducers was positioned across the beam path, and custom software automatically calculated the attenuation coefficient of the water in the beam column. This was then used to correct for the attenuating effect of cavitation on the power being measured. In addition to correcting for sources of error associated with commercial devices, the setup can easily be constructed for a much lower cost using existing, off-the-shelve components found typically in the laboratory environment. The system may also be employed for research on the effects of water borne phenomena associated with the application of ultrasound in a fluid medium.

Key words: therapeutic ultrasound; calibration; radiation force balance; acoustic cavitation; attenuation; acoustic streaming.

1. INTRODUCTION

For the past half century the field of therapeutic ultrasound (TUS) has continued to grow, where presently hundreds of research centers and universities world-wide are working to develop and improve applications in the fields of oncology, vascular disease, physical therapy, hemorrhage control, and even animal husbandry. Whereas non-focused, low intensity exposures are already being used in the clinic for healing and to enhance local transdermal

delivery, high intensity focused ultrasound (HIFU) is now becoming more accepted for non-invasive ablative therapy of uterine fibroids, prostate cancer and breast cancer [1].

The measurement of power output levels for both diagnostic and therapeutic ultrasound equipment has become increasingly important in determining exact patient exposure levels. Since the Radiation Control for Health & Safety Act of 1968 and the 1976 Medical Device Amendments to the Food and Drug Administration (FDA) Act became effective, all manufacturers of ultrasound equipment are required to submit information regarding their exposure levels and other related information. Every six months, hospitals must test output power and the general safety of their ultrasound equipment in order to maintain their accreditation. A variety of factors may contribute to deviations in output power levels. These include ambient factors such as temperature and humidity, frequency of use, and power levels employed during treatment [2].

The most important characteristic to be measured of any ultrasound device is the acoustic power, defined as the acoustic energy emitted per unit time, where the accepted SI unit for power is the watt (W). Although it does not provide information in terms of how the acoustic pressure or intensity is distributed within an ultrasound beam, it is still regarded as an essential characteristic for the assessment of safety of any ultrasound exposure [3]. A variety of methods exist for measuring the acoustic power output from an ultrasound device. These include direct measurements using piezoelectric hydrophones [4], which can be scanned through an ultrasound field to provide spatial energy distributions. Less expensive solid state devices also exist, comprised of polyvinylidene difluoride (PVDF) that utilize the pyroelectric effect [5] or semiconductor strain gauges [6]. Indirect measurement procedures are also being developed based on thermal test objects such as tissue mimicking materials (TMM). The importance of the procedures is that they provide estimates of *in situ* exposures; information directly related to the safety of these devices [3]. One such procedure involves the use of non-invasive thermography to measure spatial temperature elevations in polyacrylimide/albumin phantoms [7]. Recently, a new generation TMM was developed for characterizing HIFU exposures in soft tissues. Comprised of hydrogel with the addition of aluminum oxide particles and other components, this TMM allows for the incorporation of multiple thermocouples for simultaneous monitoring [8].

Although a variety of novel methods are being proposed and developed for measuring the power generated by ultrasound systems, today the standard is still based on the acoustic radiation force (F_{AR}). This is defined as the time-averaged force that an acoustic field exerts on an object intercepting that field, either in full or in part. If the target on which the force is exerted is larger than the cross-sectional area of the ultrasound beam, then the relationship between the force and the acoustic power, W, of the beam can be stated as [3, 9]:

$$F_{AR} = W/c, \tag{1}$$

where c is the speed of sound in the test medium, which is typically water. The sensitivity of this technique, according to equation 1 is 69 mg force per watt, and best applicable in the case of a plane wave. Deviations from a plane wave, in the case of divergent beams or highly

focused beams can significantly increase the degree of uncertainty in measurements [3]. Acoustic radiation forces will arise when acoustic waves propagate in a dissipative medium, where a transfer of momentum from the wave to the medium occurs. This results in a body force in the direction of the propagating wave [9, 10]. For a perfect absorbing target, the radiation force will be half that of a perfectly reflecting target [11].

Existing ultrasound power meters for calibration work on the principle of the radiation force method [12]. In short, a conical (i.e. non-reflecting) target is positioned in a vessel containing degassed water, which sits upon an electronic scale. The transducer to be calibrated is held in position with a stand and clamp with the face of the transducer below the waterline, directly above the cone. The transducer's radiant power is converted to a downward force (i.e. weight] on the target cone, which is transferred via the cone support assembly to the electromechanical load cell of the balance. The digital readout is in standard ultrasound units of watts.

In addition to being expensive [13], these devices require that degassed water be used in order to eliminate the effects of acoustic cavitation. Acoustic cavitation bubbles can attenuate an ultrasound beam [14], and hence, diminish the ultrasound power arriving at the target [9]. The attenuating effects of cavitating bubbles can further be problematic, where this attenuation can generate acoustic streaming, the bulk movement of fluid caused by an ultrasound wave [10]. Acoustic streaming can generate an additional force on a target in an acoustic radiation force based device, significantly increasing the measurements and, consequently rendering them inaccurate [9, 15]. Degassed water is not always available at the time of testing. And even if devices exist for degassing, it is extremely difficult to successfully degas water to the point where cavitation will completely be eliminated.

In the present study, the effects of acoustic cavitation and acoustic streaming on deviations in power measurements using the radiation force balance method were investigated for a standard commercial TUS device. A simple and inexpensive calibration system was then built and evaluated based on these results that included straightforward and effective ways to eliminate these effects and subsequently render the measurements more accurate.

2. MATERIALS AND METHODS

2.1 Experimental setup

An experimental setup was designed and built as previously described [9, 16]. A non-reflecting target in a (14 liter) water tank (L = 35 cm; W = 20 cm; H = 20 cm) was suspended from a Scout Pro analytical balance (Ohaus, Columbia, MD), with a sensitivity of 0.1 gr. The target consisted of a 8 cm × 8 cm (1 cm thick) Aptflex 28 acoustic absorber (Precision Acoustics Ltd., Dorchester, UK). The projected surface of the target was substantially larger than the surface area of the TUS transducer (5 cm^2); a requirement for implementing the radiation force technique [3]. The tank was filled with non-degassed tap water and experiments carried out a room temperature. The TUS transducer was positioned below the water line with a standard laboratory clamp. The setup appears in figure 1.

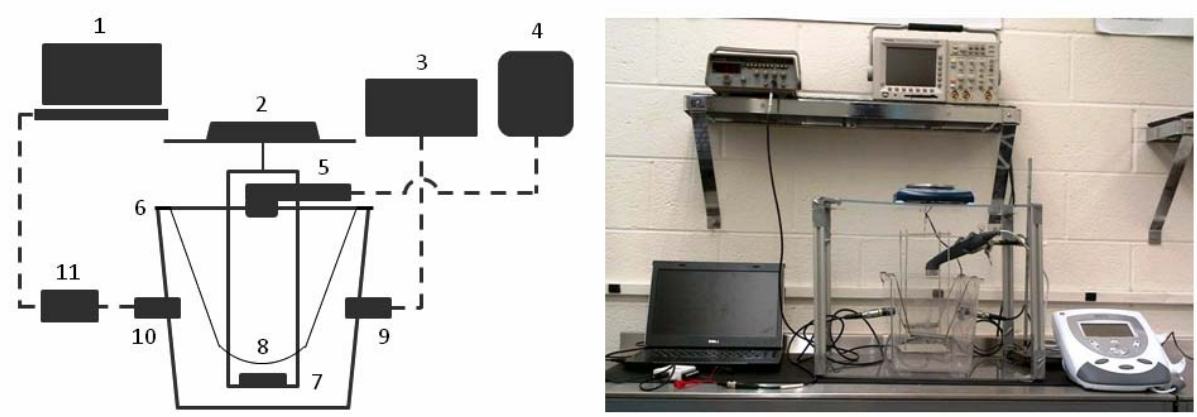

Figure 1. Experimental setup for calibrating the ultrasound transducers: Left: 1 – laptop computer; 2 – electronic balance; 3 – function generator; 4 – TUS generator; 5 – TUS transducer; 6 – water tank; 7 – absorbing target; 8 – acoustic permeable membrane; 9 – transmitting transducer; 10 – receiving transducer; 11 – analog/digital convertor. Right: Digital image of the setup

For all experiments, an Intelect Transport commercial TUS system (Encore Medical Tech., Los Angeles, CA) was used, operating at 1 and 3.3 MHz, with a maximal power of 12.5 W. All exposures were carried out in continuous mode and at powers from 0 to 10 W. For all measurements, the scale was turned on and the reading on the display was allowed to stabilize. The scale was then tared and the ultrasound exposure was turned on. The reading on the scale was translated into power, P, [W], using the following equation [15]:

$$P = \Delta m \cdot g \cdot c/(1 + r^2), \quad (2)$$

where Δm is the change in mass measured on the balance in response to the radiation force generated by the ultrasound exposure [kg], g is gravity [9.8 ms^{-1}], c is the speed of sound in water [1500 ms^{-1}], and r is the reflection coefficient of the target. For complete non-reflection with the target, $r = 0$, equation 2 can be written simply as:

$$P = \Delta m \cdot g \cdot c. \quad (3)$$

2.2 Initial evaluation

The initial evaluation of the experimental calibration setup consisted of measurements at both frequencies (1 and 3.3 MHz), and in the range of powers from 0 to 10 W, at increments of 0.5 W. Each measurement was repeated 5 times, and means and standard deviations calculated.

2.3 Effects of acoustic streaming

In order to determine the contributions of acoustic streaming, a 0.013 mm thick silicon acoustic permeable membrane (McMaster Carr, Atlanta, GA), 8 cm × 8 cm, was suspended 1 cm above the absorber [9]. Measurements, with and without the membrane, were taken at 0, 2.5, 5, 7.5 & 10 W, at 1 and 3.3 MHz (n = 5), and means and standard deviations calculated.

2.4 Acoustic cavitation activity

Investigations were carried out to characterize the activity of acoustic cavitation. A 1 MHz A-303S-SU immersion ultrasound imaging transducer (13 mm element size) (Olympus, Waltham, MA) was positioned on the side of the tank, pointing inward towards the center of the ultrasound beam. The vertical position of the transducer was chosen to be precisely at the halfway point between the face of the TUS and the absorber. The transducer was connected to a TBS1000 Tektronix digital oscilloscope (Tektronix Inc., Beaverton, OR). Signals were collected at a sampling rate of 250 MB s^{-1}, and processed in FFT mode. Exposures were carried out at 5 and 10 W. Ten 30-s samples were collected at both 1 and 3.3 MHz. The data, in CSV format, was then transferred by floppy disc to a desktop computer. MATLAB™ software was used to extract the voltage values at the fundamental frequencies (i.e. of the TUS exposures), as well as at the 2nd, 3rd, and 4th harmonics, which are used to characterize non-inertial cavitation activity [17]. This data was then transferred to a digital spread sheet, where the mean peak-to-peak voltages were calculated for each 30-s measuring period. Note: half harmonic emissions were not used for this purpose, seeing that compared to the other wavelengths, emissions at this wavelength were not consistently detected.

2.5 Attenuation effects of acoustic cavitation

In order to determine the attenuating effects of the cavitation bubbles in the ultrasound beam, a second 1 MHz, imaging transducer was positioned directly opposite the first, on the other side of the tank. A GFG-8020H function generator (GW Instek, Taiwan) was used to generate a 4.3 V (peak-to-peak), 1 MHz signal through one of the transducers (designated as the transmitting transducer). The signal received by the second (receiving) transducer was observed via the oscilloscope. Both the transmitted and received signals were transferred to a desktop PC computer using a USB-6008 analog to digital converter (Dataq Instruments, Inc., Akron, OH). MATLAB™ software was used to plot, in real time, the respective amplitudes of the transmitted (V_{in}) and received (V_{out}) signals as a function of time. Initially, measurements were carried out of the attenuation of the water (without ultrasound) between the two transducers (equation 5). The TUS transducer was then turned on and the attenuation of the water in the ultrasound beam was determined (equation 4). These procedures are summarized in figure 2.

The acoustic attenuation coefficient (dB/cm/MHz) of the water column in the ultrasound beam was calculated as:

$$\alpha = \ln(V_{out}/V_{in})/D + \alpha_{water}, \quad (4)$$

where D is the diameter of the ultrasound beam, and

$$\alpha_{water} = \ln(V_{out}/V_{in})/l, \quad (5)$$

where l is the distance between the two ultrasound imaging transducers, and V_{out} and V_{in} are the transmitted and received signals, respectively, when the TUS transducer was off. This measurement was carried out prior to each attenuation measurement. For both attenuation

measurements, with and without the TUS transducer on, the values were averaged over a duration of 30 s.

Measurements were carried out at both 1 and 3.3 MHz, at 0, 2.5, 5, 7.5 & 10 W cm^{-2} (n = 5), and means and standard deviations calculated. This procedure was repeated with and without a 30 s period of aeration prior to the measurements. A MATLAB™ program, with graphic user interface, was implemented to automatically calculate the attenuation coefficient.

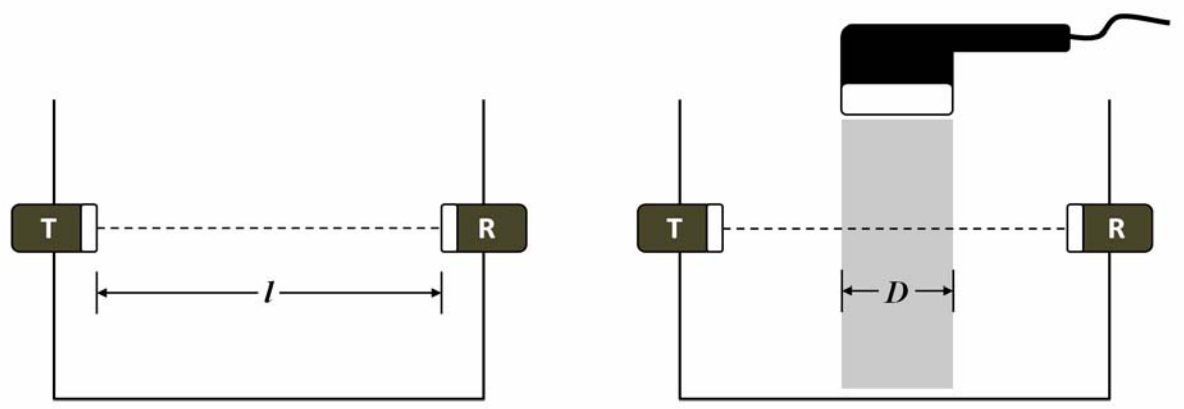

Figure 2. A schematic depiction of the factors involved for determining the attenuation coefficient of the water (left), and the water column in the ultrasound beam (right): T – transmitting diagnostic ultrasound transducer; R – receiving diagnostic ultrasound transducer; *l* – distance between the two transducers; *D* – diameter of the water column. V_{in} and V_{out} were measured at T and R, respectively, and employed in equations 4 and 5

2.6 Corrected measurements

The initial evaluation was repeated, where measurements were taken at both frequencies, from 0 to 10 W, and at increments of 0.5 W. Each measurement was repeated 5 times. This time, however, the water was aerated prior to the measurements (as described above) and the acoustic permeable membrane was positioned just above the absorber (as previously described). The attenuation of the water in the ultrasound beam was also measured each time (as described above).

In a homogenous medium with a known acoustic attenuation coefficient, the intensity (*I*) at any distance (*d*) from a source can be calculated according to [18]:

$$I = I_o \cdot e^{-2ad}, \tag{6}$$

where I_o is the intensity at the source and α is the attenuation coefficient [dB/cm/MHz].

Seeing that the intensity is the spatial averaged power ($I = P/A$), where the surface area of the transducer, *A*, is constant, the measured power was corrected for the effects of attenuation by combining equations 3 and 6:

$$P_{cor} = \Delta m \cdot g \cdot c \cdot e^{2ad}, \tag{7}$$

where α was the measured attenuation coefficient [dB/cm/MHz] of the water in the ultrasound beam and *d* was the distance (11 cm) between the TUS transducer and the target.

2.7 Statistical Analysis

For all comparisons of experimental group data, a pair wise t-test was used, assuming unequal variances. Statistically significant differences in group means were determined according to a P-value of 0.05 or less.

3. RESULTS

3.1 Initial evaluation

The first experiment carried out was designed to determine if differences exist between the measured power and the power indicated on the device at each frequency. At 3.3 MHz significant differences were not found over the entire range of powers evaluated. At 1 MHz significant differences were observed from 1.5 to 10 W. Over this range of powers, the mean difference increased in a linear manner from 0.3 to 5.5 W, indicating a mean discrepancy of approximately 50% at the highest power. The results are summarized in figure 3.

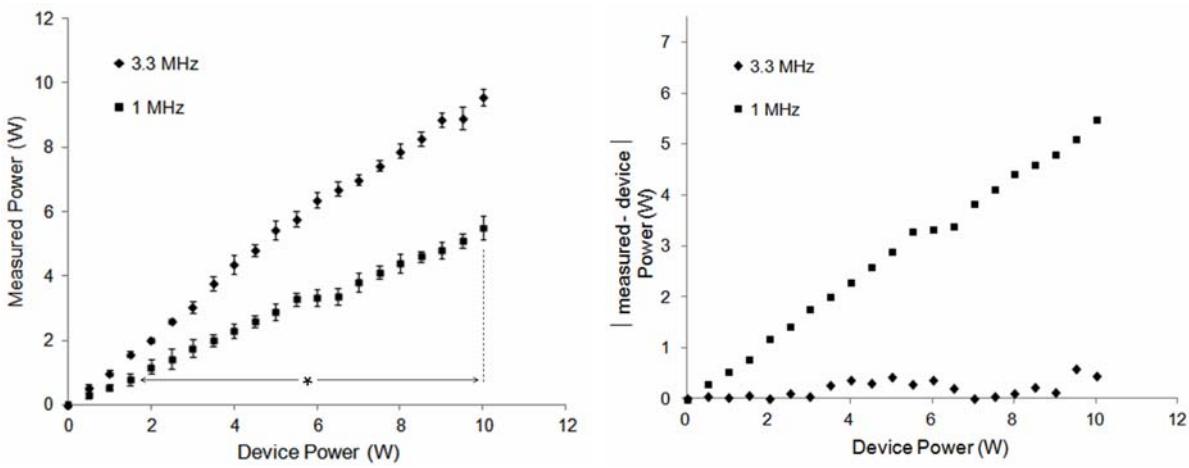

Figure 3. Results from the initial evaluation of the calibration setup. (Left) At 3.3 MHz measured powers were not found to be significantly different than the device power over the entire range of powers evaluated. At 1 MHz, measured powers were significantly lower than the device power from 1.5 to 10 W. Values are group means (n = 5); error bars are standard deviations. (Right) Absolute values of the differences between the measured and device powers plotted against the device power. Values are group means (n = 5)

3.2 Effects of acoustic streaming

This experiment was carried out was determine if acoustic streaming had an effect on the measured power. At 3.3 MHz, significant differences were not found with and without streaming, over the entire range of powers evaluated. At 1 MHz significant differences were observed at all the powers evaluated. Over this range of powers, the mean difference increased in a linear manner according to the equation:

$$P_{wo} - P_w = 0.41P_D, \qquad R^2 = 0.9995, \tag{8}$$

where P_{wo} is the measured power without the membrane, P_w is the measured power with the membrane, and P_D is the device power. The results are summarized in figure 4.

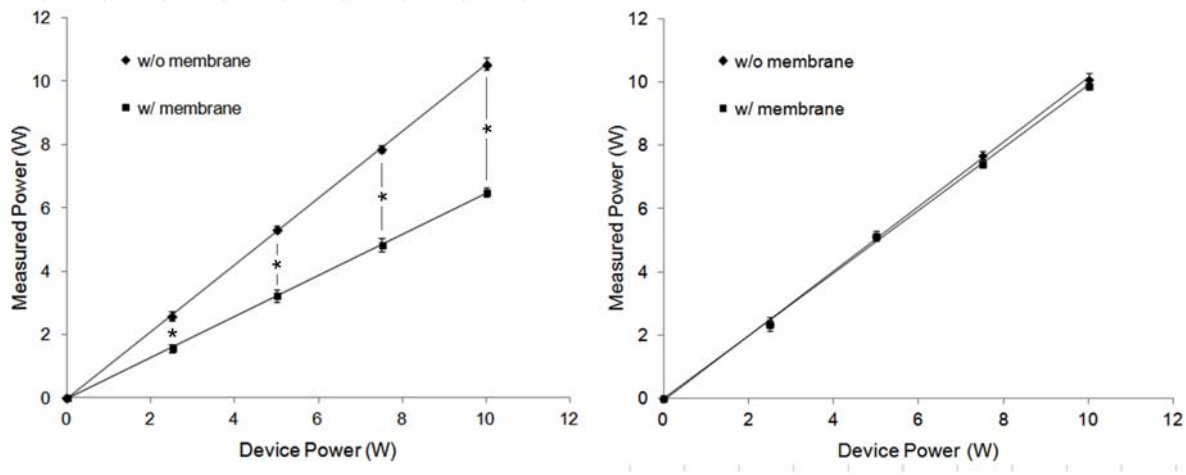

Figure 4. Results on the effects of acoustic streaming. At 3.3 MHz (right) significant differences were not found between the measured power, with and without the acoustic permeable membrane, at any power evaluated. At 1 MHz (left) significant differences were observed between the measured power, with and without the acoustic permeable membrane, at all the evaluated powers. The difference between the two increased linearly as a function of the device power. Values are group mean (n = 5); error bars are standard deviations

3.3 Acoustic cavitation activity

At 1 MHz, 2nd (2 MHz), 3rd (3 MHz), and 4th (4 MHz) harmonics were clearly observed at both powers evaluated. Whereas a trend of increasing amplitudes (relative to the fundamental) was found for each harmonic at 10 W compared to 5 W, the values were not significantly different for any of the harmonics. Similarly, for each power, the relative amplitude for the 2nd harmonic was observed to be greater than for the 3rd harmonic, and the 3rd harmonic greater than the 4th harmonic. However, these differences were not statistically significant. Harmonics were not detected at 3.3 MHz for all powers. Representative harmonic distributions for each power are shown in figure 5, as well as a quantitative analysis for group means.

3.4 Attenuation effects of acoustic cavitation

At 3.3 MHz, the addition of aeration to the treatment tank was not found to significantly affect the attenuation coefficient of the water column in the ultrasound beam during the exposures at any of the powers evaluated. Significant increases in attenuation were also not found to occur as the power increased over the entire range of powers evaluated, with or without aeration. Conversely, at 1 MHz, aeration was found to increase the attenuation coefficient at all the powers evaluated, where for both conditions (with and without aeration) the attenuation (α) increased with an increase in power (P):

<u>with aeration:</u> $\alpha\,[\mathrm{dB{\cdot}cm^{-1}{\cdot}MHz^{-1}}] = 0.153 + 0.004P\,[\mathrm{W}], \quad R^2 = 0.989;$ (9)

<u>without aeration:</u> $\alpha\,[\mathrm{dB\ cm^{-1}\ MHz^{-1}}] = 0.151 + 0.0033P\,[\mathrm{W}], \quad R^2 = 0.994.$ (10)

Over the entire range of powers evaluated, the attenuation coefficient of the water column at 1 MHz without aeration was found to be greater than at 3.3 MHz. The results appear in figure 6.

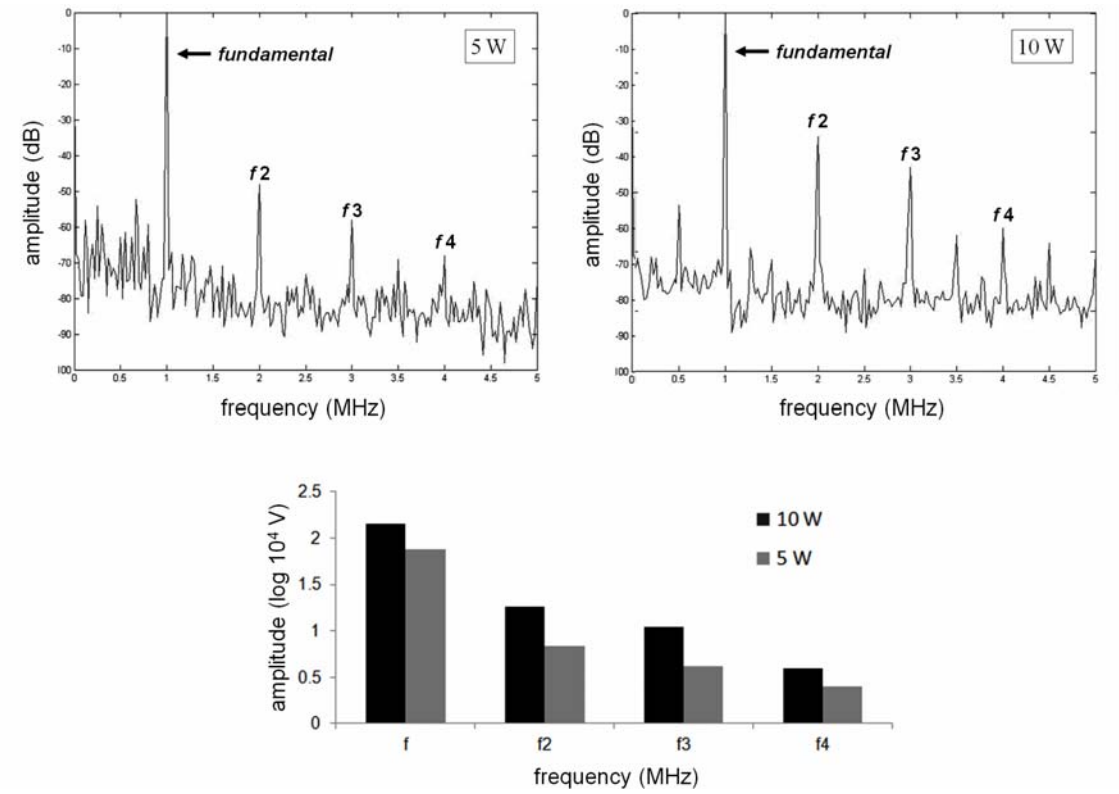

Figure 5. Upper images: Representative harmonic distributions for 5 W (left) and 10 W (right) for 1 MHz. Below: A quantitative analysis of the data for both powers (n = 10). Although trends are seen in the relative differences in the amplitudes of the fundamental frequencies and their respective harmonics, statistically significant differences were not found. Bars are group means. Standard deviations were calculated for all mean values. However, these were so low as to not be discernible on the graph. Harmonics were not detected at 3.3 MHz at either power.

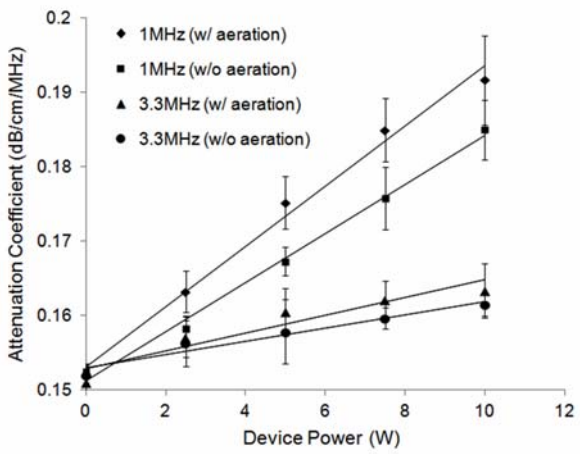

Figure 6.

Attenuation of the water column in the ultrasound beam, for both 1 and 3.3 MHz, with and without aeration. Aeration was found to increase the attenuation coefficient at 1 MHz at all powers, but not at 3.3 MHz. Overall, the attenuation coefficient was greater at 1 MHz than at 3.3 MHz for all powers evaluated. Values are group mean (n = 5); error bars are standard deviations

3.5 Corrected measurements

With the acoustic permeable membrane in place and when correcting for the attenuation of the water in the ultrasound beam (equation 7), the measured power was not found to be significantly different than the device power over the entire range of powers evaluated (0 to 10 W), and at either frequency. The results appear in figure 7.

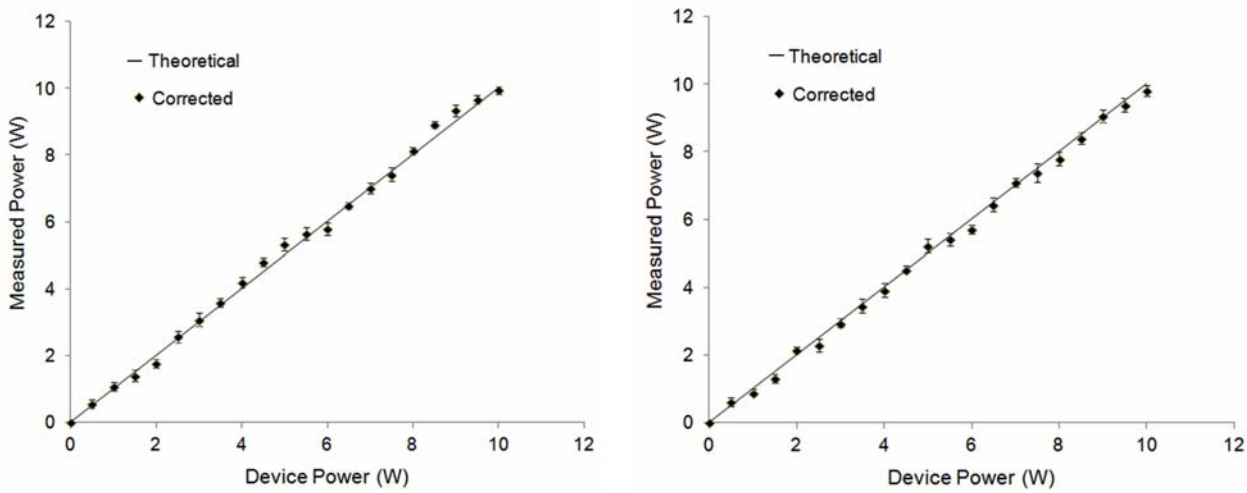

Figure 7. Corrected measured power versus the device power for 1 MHz (left) and 3.3 MHz (right). The measured powers were corrected by incorporating the attenuation of the water in the ultrasound beam, itself a function of the power. An acoustic permeable membrane was also used to eliminate the effect of acoustic streaming. The solid line in each graph represents a theoretical condition where the measured power equals the device power. Values are group means (n = 5); error bars are standard deviations

4. DISCUSSION

The present study describes a systematic investigation in to how water-associated acoustic phenomena may adversely affect radiation force based calibration devices for TUS transducers, and as a result render them inaccurate. This knowledge is then used to propose a straightforward and accurate methodology for calibration, based on simple components typically found in the laboratory environment. The proposed methodology also incorporates a departure from the traditional approach. Typically the water in a test tank is degassed as best as possible in order to minimize the attenuation of the water in the ultrasound beam due to cavitating bubbles [19]. Instead, the medium is saturated with air prior to measurements and the attenuation is measured and used to correct the measurements. The effects of acoustic streaming are eliminated by simply placing an acoustic permeable membrane above a non-reflecting target.

Acoustic cavitation and acoustic streaming are the two main phenomena occurring as a result of applying an ultrasound exposure in free field (i.e. in unconfined water) [11]. The two are also inter-related, where cavitation must occur in order for there to be streaming. Acoustic cavitation can broadly be defined as the growth, oscillation, and collapse of small stabilized gas bubbles in response to the varying pressure field of ultrasound wave. The bubbles can

oscillate stably (i.e. non-inertial cavitation), or grow beyond their resonant size and collapse violently (known as inertial cavitation) [20]. The presence of cavitating bubbles will attenuate an ultrasound wave, where the attenuation will be proportional to the bubble density [21].

In the present study, cavitation was detected at powers as low as 2 W, for the 1 MHz exposures. These results are consistent with the observations that the measured power was found to be significantly lower than the device power, at powers as low as 1.5 W. Conversely, at 3.3 MHz, cavitation activity was not detected even at the highest power evaluated, 10 W, where statistically significant differences were not found between the measured and device power. These results are consistent with the predictive relationship of frequency and the intensity threshold for the onset of cavitation using the mechanical index (MI). The MI (= $PNP/f^{1/2}$), used to assess the safety of medical ultrasound devices, states that the higher the center frequency (f [MHz]) of the ultrasound exposure, the greater the peak negative pressure (PNP [MPa]) required for cavitation to occur [22]. Furthermore, an earlier study employing exposures in free-field at 1 MHz reported that cavitation was observed at powers as low as 2.5 W (i.e. at a spatial averaged intensity of 0.5 Wcm^{-2} with a transducer possessing a surface area of 5 cm^2) [16]. In a follow up study employing exposures at 3 MHz, cavitation was not observed even at a power of 11 W (i.e. at a spatial averaged intensity of 2.2 Wcm^{-2} with a transducer possessing a surface area of 5 cm^2) [23]. Indeed, an even earlier study had reported the free-field threshold for cavitation at 3 MHz to be above 3 Wcm^{-2} [24]. This would be equivalent to 15 W in the present study, where the transducer had a surface area of 5 cm^2, and therefore 50% greater than the maximum power evaluated, where cavitation was still not detected.

Attenuation of an ultrasound wave can be attributed to either absorption or scattering as it propagates through a medium. For an ultrasound wave propagating through a typical soft tissue, the absorption of energy will be converted into heat, where the scattering is the portion of the wave that is redirected [11]. Regarding the attenuation of ultrasound due to the presence of cavitation, it presumably would be due primarily to scattering because of the high echogenicity of the gas-filled bubbles. Indeed, the clinical practice of using gas-filled microbubble-based contrast agents for delineating blood vessels for diagnostic ultrasound is based on the very principle that strong echos are generated, and the incident wave is, for the most part, attenuated [14]. In one study investigating the effects of cavitation on energy attenuation, as the amount of water was increased in an ultrasonic cleaning vessel (increasing the amount of bubbles in the path of the ultrasound wave) a decrease was observed in the pressure field at a target. These results were supported by numerical analysis, which showed the energy dissipation to be directly proportional to the number of bubbles [25].

The experimental results showing an increase in attenuation with an increase in power, at 1 MHz, was apparently due primarily to an increase in the number of cavitation bubbles as the power was increased. This is supported by the observation that a significant increase in attenuation occurred as the power increased. This phenomenon was enhanced when aeration was supplied to the system, where the rate of increase in the attenuation with power was measured to be 20% higher with aeration than without it. The number and the availability of

gas micronuclei are among the factors that can affect the activity of acoustic cavitation, including an increase in activity in proportion to the amount of dissolved gas and/or micronuclei [26]. Aeration was supplied to water of the system prior to each measurement in order to consistently saturate the medium with cavitation nuclei. This was a requirement for the procedure that was eventually developed where the relationship between the applied power and the attenuation of the medium was required to be predictable.

Acoustic streaming is the bulk movement of fluid in response the application of an ultrasound wave, occurring as a transfer of momentum from the absorption of energy. [27]. The acoustic streaming velocity will be proportional to the absorption coefficient of the medium and the intensity of the ultrasound exposure, and inversely proportional to the bulk viscosity and speed of sound of the medium [28]. A number of clinical applications have been proposed employing the detection of induced streaming, for example with ultrasound Doppler imaging. These include differentiating between solid tumors and fluid filled cysts [29, 30], and between stagnant and flowing blood [28]. Using exposures in free-field comparable to those employed in the present study, Frenkel et al [31] reported a linear relationship between the intensity of the exposures and the streaming velocity. Using particle image velocimetry (PIV), they observed a peak streaming velocity of 2.5 cm s^{-1} at 10 W (i.e. at a spatial averaged intensity of 2 W cm^{-2} with a transducer possessing a surface area of 5 cm^2).

The effect of acoustic streaming on power measurement using the radiation force balance technique has previously been reported. One study compared the differences observed between a radiation force balance with an absorbing target and a polyethylene terephthalate (PET) sensor, where the latter was not affected by the force generated by the induced streaming. The power measured with the radiation force balance was shown to be the sum of the true power being sensed and the power component generated by the streaming [15], where the latter is the result of the dynamic pressure generated by the flow [32]. Another study using HIFU exposures showed an 18% decrease in measured power when an acoustic permeable membrane was placed 1 cm above an absorbing target [9]. In the present study, an additive effect of acoustic streaming on the radiation force measured was not detected for the 3.3 MHz exposures, apparently due to the absence of acoustic cavitation. At 1 MHz, however, where cavitation was present, acoustic streaming did occur, and increased with applied power. This was determined indirectly where an increase in the disparity between measured power with and without the acoustic permeable membrane increased as the device power was increased. On average, over the range of powers evaluated, a decrease in power of 41% was observed with the acoustic permeable membrane. The increase in disparity of these measurements with applied power is to be expected. Both an increase in applied power and attenuation [28], which itself was found to increase with power, will result in an increase in the streaming velocity, and hence the force generated on the target.

In summary, the present study described the manner by which phenomena generated by an ultrasound wave in free-field can render radiation force balance measurements of acoustic power inaccurate. This was demonstrated for the 2 frequencies typically used for physical therapy ultrasound treatments. At the higher frequency, acoustic cavitation does not occur in

the range of powers available for commercial devices. And as a consequence, deviations were not observed between the measured power and the power indicated on the device. On the other hand, cavitation was present for the lower frequency over almost the entire range of powers evaluated. The attenuating effect of the cavitating bubbles was shown to decrease the measured power; the streaming generated by the attenuation was conversely shown to increase it. Overall, the effects of attenuation were greater than those of the streaming, and the net measured power was on average 50% lower than the power supplied by the device.

In the process of investigating these phenomena a simple, straightforward procedure for correcting their effects on power measurement was proposed, and subsequently demonstrated to be accurate and effective. The device was comprised of components typically found in the laboratory environment, and at a fraction of the cost of a typical commercial calibration device. Future studies will look at the potential benefits of additional modifications of the procedure. This includes lowering the effective duty factor (EDF); the product of pulse duration and the pulse repetition frequency. A lower EDF would correspondingly lower the temporal-average power and, hence, cavitation activity and the streaming that results from it. For HIFU exposures, where cavitation and streaming become more prominent, a lower EDF was shown to have a measurable effect for improving calibration efficiency [9]. Investigations could also be carried out on decreasing the distance between the acoustic permeable membrane and the target (to further minimize the effect of streaming).

One limitation of the proposed procedure is that it assumed that the attenuation coefficient of the water within the ultrasound beam was uniform from the face of the TUS transducer until the absorber and equal to the value measured at the half-way point between the two. Preliminary trials had indicated that this was the most accurate way to represent the attenuation, where it would not be practical or cost-effective to carry out multiple measurements simultaneously throughout the water column. Furthermore, the center frequency of the transmitting and receiving imaging transducers was not necessarily ideal for measuring the attenuation of the cavitating bubbles. These however were used because of their availability and low cost. Overall, despite these limitations, the device was still shown to be accurate and effective for its designed purpose. Ultimately, its design is meant to be conceptual, and investigators are expected to modify and improve on it based on the application, and the available equipment and resources.

ACKNOWLEDGEMENTS

The authors would like to thank Mr. Don Smolley and Mr. Afshin Nabili for their help in constructing various components of the experimental system. This research was funded in part by an internal grant from Catholic University of America.

REFERENCES

1. Frenkel V (2008) Ultrasound mediated delivery of drugs and genes to solid tumors. *Adv Drug Deliv Rev* 60(10):1193-1208.
2. Ferrari CB, Andrade MA, Adamowski JC, & Guirro RR (2010) Evaluation of therapeutic ultrasound equipment performance. *Ultrasonics* 50(7):704-709.
3. Zeqiri B (2007) Metrology for ultrasonic applications. *Prog Biophys Mol Biol* 93(1-3):138-152.
4. Lewin PA (2010) Nonlinear Acoustics in Ultrasound Metrology and other Selected Applications. *Phys Procedia* 3(1):17-23.
5. Harris GR, Preston RC, & Dereggi AS (2000) The impact of piezoelectric PVDF on medical ultrasound exposure measurements, standards, and regulations. *IEEE Trans Ultrason Ferroelectr Freq Control* 47(6):1321-1335.
6. Bindal VN, Singh VR, & Singh G (1980) Acoustic power measurement of medical ultrasonic probes using a strain gauge technique. *Ultrasonics* 18(1):28-32.
7. Patel PR, *et al.* (2008) In vitro and in vivo evaluations of increased effective beam width for heat deposition using a split focus high intensity ultrasound (HIFU) transducer. *Int J Hyperthermia*:1-13.
8. King RL, *et al.* (2011) Development and characterization of a tissue-mimicking material for high-intensity focused ultrasound. *IEEE Trans Ultrason Ferroelectr Freq Control* 58(7):1397-1405.
9. Maruvada S, Harris GR, Herman BA, & King RL (2007) Acoustic power calibration of high-intensity focused ultrasound transducers using a radiation force technique. *J Acoust Soc Am* 121(3):1434-1439.
10. Nightingale KR, Nightingale RW, Palmeri ML, & Trahey GE (2000) A finite element model of remote palpation of breast lesions using radiation force: factors affecting tissue displacement. *Ultrason Imaging* 22(1):35-54.
11. O'Brien WD, Jr. (2007) Ultrasound-biophysics mechanisms. *Prog Biophys Mol Biol* 93(1-3):212-255.
12. Lewin PA, Barrie-Smith N, Ide M, Hynynen K, & Macdonald M (2003) Interlaboratory acoustic power measurement. *J Ultrasound Med* 22(2):207-213.
13. Muttakin I, *et al.* (2011) Low cost design of precision medical ultrasound power measurement system. *Int'l J Circuits Sys Signal Proc* 5(6):672-682.
14. Miller DL, *et al.* (2008) Bioeffects considerations for diagnostic ultrasound contrast agents. *J Ultrasound Med* 27(4):611-632; quiz 633-616.
15. Kikuchi T, Sato S, & Yoshioka M (2004) Quantitative Estimation of Acoustic Streaming Effects on Ultrasonic Power Measurement. *IEEE UFFC*:2197-2200.
16. Frenkel V, Kimmel E, & Iger Y (1999) Ultrasound-induced cavitation damage to external epithelia of fish skin. *Ultrasound Med Biol* 25(8):1295-1303.
17. O'Neill BE, *et al.* (2009) Pulsed high intensity focused ultrasound mediated nanoparticle delivery: mechanisms and efficacy in murine muscle. *Ultrasound Med Biol* 35(3):416-424.
18. Lele PP (1980) Induction of deep, local hyperthermia by ultrasound and electromagnetic fields: problems and choices. *Radiat Environ Biophys* 17(3):205-217.
19. Johns LD, Straub SJ, & Howard SM (2007) Analysis of effective radiating area, power, intensity, and field characteristics of ultrasound transducers. *Arch Phys Med Rehabil* 88(1):124-129.
20. Kimmel E (2006) Cavitation bioeffects. *Crit Rev Biomed Eng* 34(2):105-161.
21. Duraiswami R, Prabhukumar S, & Chahine GL (1998) Bubble counting using an inverse acoustic scattering method. *J Acoust Soc Am* 104(5):2699-2717.

22. Apfel RE & Holland CK (1991) Gauging the likelihood of cavitation from short-pulse, low-duty cycle diagnostic ultrasound. *Ultrasound Med Biol* 17(2):179-185.
23. Frenkel V, Kimmel E, & Iger Y (2000) Ultrasound-induced intercellular space widening in fish epidermis. *Ultrasound Med Biol* 26(3):473-480.
24. Hill CR (1971) Ultrasonic exposure thresholds for changes in cells and tissues. *J Acoust Soc Am* 52(2):667-672.
25. Nomura S & Nakagawa M (2001) Analysis of an ultrasonic field attenuated by oscillating cavitation bubbles. *Acoust Sci & Tech* 22(4):283-291.
26. Barnett SB, *et al.* (1994) Current status of research on biophysical effects of ultrasound. *Ultrasound Med Biol* 20(3):205-218.
27. Nightingale KR & Trahey GE (2000) A finite element model for simulating acoustic streaming in cystic breast lesions with experimental validation. *IEEE Trans Ultrason Ferroelectr Freq Control* 47(1):201-214.
28. Shi X, Martin RW, Vaezy S, & Crum LA (2002) Quantitative investigation of acoustic streaming in blood. *J Acoust Soc Am* 111(2):1110-1121.
29. Soo MS, *et al.* (2006) Streaming detection for evaluation of indeterminate sonographic breast masses: a pilot study. *AJR Am J Roentgenol* 186(5):1335-1341.
30. Nightingale KR, Kornguth PJ, & Trahey GE (1999) The use of acoustic streaming in breast lesion diagnosis: a clinical study. *Ultrasound Med Biol* 25(1):75-87.
31. Frenkel V, Gurka R, Liberzon A, Shavit U, & Kimmel E (2001) Preliminary investigations of ultrasound induced acoustic streaming using particle image velocimetry. *Ultrasonics* 39(3):153-156.
32. Campbell M, Cosgrove JA, Greated CA, Jack S, & J.D. R (2000) Review of LDA and PIV applied to the measurement of sound and acoustic streaming. *Optics Laser Tech* 32:629-639.